Development 125, 3895-3903 (1998)
Printed in Great Britain © The Company of Biologists Limited 1998
DEV3804

Cell-type-specific rescue of myosin function during *Dictyostelium* development defines two distinct cell movements required for culmination

Tung-Ling L. Chen, Wendy A. Wolf and Rex L. Chisholm*

Department of Cell and Molecular Biology, Northwestern University Medical School, 303 E. Chicago Avenue, Chicago, IL 60611, USA
*Author for correspondence (e-mail: r-chisholm@nwu.edu)

Accepted 13 July; published on WWW 7 September 1998

SUMMARY

Mutant *Dictyostelium* cells lacking any of the component polypeptides of myosin II exhibit developmental defects. To define myosin's role in establishing *Dictyostelium*'s developmental pattern, we have rescued myosin function in a myosin regulatory light chain null mutant (mlcR$^-$) using cell-type-specific promoters. While mlcR$^-$ cells fail to progress beyond the mound stage, expression of RLC from the prestalk promoter, ecmA, produces culminants with normal stalks but with defects in spore cell localization. When GFP-marked prestalk and prespore cells expressing ecmA-RLC are mixed with wild-type cells, the mislocalization of prestalk cells, but not prespore cells, is rescued. Time-lapse video recording of ecmA-RLC cells showed that the posterior prespore zone failed to undergo a contraction important for the upward movement of prespore cells. Prespore cells marked with green fluorescent protein (GFP) failed to move toward the tip with the spiral motion typical of wild type. In contrast, expression of RLC in prespore cells using the psA promoter produced balloon-like structures reminiscent of sorocarps but lacking stalks. GFP-labeled prespore cells showed a spiral movement toward the top of the structures. Expression of RLC from the psA promoter restores the normal localization of psA-GFP cells, but not ecmA-GFP cells. These results define two distinct, myosin-dependent movements that are required for establishing a *Dictyostelium* fruiting body: stalk extension and active movement of the prespore zone that ensures proper placement of the spores atop the stalk. The approach used in these studies provides a direct means of testing the role of cell motility in distinct cell types during a morphogenetic program.

Key words: Myosin, *Dictyostelium*, Cell movement, Culmination, GFP, Green Fluorescent Protein

INTRODUCTION

Dictyostelium amoebae respond to environmental stress by forming multicellular aggregates. These aggregates undergo a program of morphogenesis to construct a fruiting body with a stalk that supports a spore case above the substratum to facilitate spore dispersal. This morphogenetic program involves a variety of cell movements orchestrated by chemotactic signals (Durston et al., 1976; Siegert and Weijer, 1992). During aggregation, thousands of single-celled amoebae move toward an aggregation center by chemotaxis to cAMP pulses (Devreotes, 1989; Wessels et al., 1992). Following arrival in the aggregate, cells begin to differentiate down one of two major pathways ultimately leading to the formation of spores and stalk. A population of prestalk cells, defined by expression of the cell autonomous ecmA marker (pstA), sorts to the top of the mound to form a tip that acts as an organizer for the next stage of morphogenesis (Jermyn and Williams, 1991). In addition, the ecmA promoter has been shown to also drive expression of a marker gene in a second population of prestalk cells called pstO cells (Early et al., 1993). A spiraling motion is observed in the mounds as cells migrate into the tip (Clark and Steck, 1979; Elliot et al., 1993; Siegert et al., 1994). This spiral motion has been proposed to act as a vortex to drive the elongation of mounds into fingers (Clark and Steck, 1979). A similar spiral motion occurs in the anterior region of the prestalk zone of migrating slugs, which has been proposed to be organized by a three-dimensional cAMP scroll wave. The cAMP scroll wave becomes a planar wave upon entering the prespore zone where it directs the periodic forward movement of the prespore cells (Siegert and Weijer, 1992). When slugs begin culmination, formation of a stalk tube is initiated by secretion of a cellulosic sheath from a group of prestalk cells at the center of the prestalk zone (pstB) (Jermyn and Williams, 1991). As additional prestalk cells enter into the stalk tube from the top, the stalk sheath extends downward and cells in the stalk tube become vacuolated, ultimately lifting the spore mass above the substratum (Durston et al., 1976). It has been widely accepted that stalk extension provides the force that lifts the spore mass off the substratum to form fruiting bodies. At the onset of culmination, a population of anterior-like cells (ALC) moves to the rear of the slug where they begin a rotational movement (Dormann et al., 1996). These cells eventually produce the basal disc and the lower cup of the fruiting body (Dormann et al., 1996; Jermyn and Williams, 1991; Sternfeld and David, 1982). The subpopulation of ALCs that form the lower cup have been proposed to play an active role in lifting

the spore mass up the stalk tube (Sternfeld and David, 1982). Alternatively, these ALCs have been proposed to play a role in maintaining the integrity of the spore head as it moves up the stalk (Jermyn and Williams, 1991).

Myosin II plays critical roles in *Dictyostelium* development. Null mutants of myosin heavy chain (mhcA$^-$) and of either light chains (mlcR$^-$, mlcE$^-$) are defective in development (DeLozanne and Spudich, 1987; Knecht and Loomis, 1987; Chen et al., 1994, 1995). Studies using mhcA$^-$ cells have established a series of morphogenetic events that require myosin: chemotaxis during aggregation (Wessels et al., 1988), spiraling motion in mounds (Elliot et al., 1993), tip formation (Elliot et al., 1993; Traynor et al., 1994), and stalk formation (Springer et al., 1994). MlcR$^-$ cells form mounds becoming arrested morphologically at the same stage as mhcA$^-$ cells (Chen et al., 1994). MlcE$^-$ cells form mounds with varying developmental potency, half arresting at mounds, and the remainder forming aberrant fruiting bodies (Chen et al., 1995). In single-cell chemotaxis assays, mhcA$^-$ cells failed to polarize and moved with greatly reduced rates toward chemoattractants (Wessels et al., 1988), while mlcE$^-$ cells polarized normally, but showed reduced migration rates similar to mhcA$^-$ cells (Chen et al., 1995). These defects in motility seem likely to be a major factor in the abnormal development of myosin mutants.

To more precisely define the contributions of cell movement during *Dictyostelium* development, we have developed an approach to specifically alter the motile properties of cells in specific cell types during development. Myosin function and thus normal motility was selectively restored in specific differentiated cell types. To accomplish this, cell-type-specific promoters were used to drive myosin regulatory light chain (RLC) expression in cells of the prespore and prestalk A/pstO cell types during mlcR$^-$ development. The movements of the rescued cells have been followed by marking prestalk and prespore cells with green fluorescent protein (GFP) cell-type markers. These studies have defined distinct, myosin-dependent cell movements in both prespore and prestalk cells that are required for normal morphogenesis.

MATERIALS AND METHODS

DNA constructs

The ecmA promoter was derived from pEcmA-gfp (provided by Hodgkinson and Kay, MRC, Cambridge), modified through polymerase chain reaction(PCR) to remove the translation initiation codon and to generate a downstream cloning site for RLC. The ecmA-gfp expression cassette of pEcmA-gfp was cloned into pSK in order to use the universal primer on pSK as the 5′ PCR primer. A 25 nucleotide segment from 3′ of the ecmA promoter just upstream of the start codon was used to make the 3′ primer. A *Bgl*II-*Xho*I fragment containing the PCR fragment was excised from the AT cloning vector pCRII (Invitrogen, Carlsbad CA) and cloned into pDdGal-17 (Harwood and Drury, 1990) between the *Bam*HI and *Xho*I sites replacing the *lacZ* to produce the prestalk expression construct pEcmA-ΔATG. A full-length RLC cDNA was then inserted into pEcmA-ΔATG at the *Eco*RI site to produce the prestalk RLC expression construct pEcmA-RLC. A similar strategy was used to produce pPsA-RLC. The psA-gfp cassette used as PCR template was derived from pPsA-gfp provided by T. Kawata and J. Williams (University College London). A sequence from the psA promoter starting three nucleotides upstream of the ATG and extending into the junction between the psA promoter and gfp was used as the 3′ PCR primer. A single base mismatch was introduced to remove the start codon. The prespore expression construct pPsA-ΔATG was made by joining a psA promoter fragment produced by PCR with the actin 8 terminator on pPsA-gfp. A full-length RLC cDNA was cloned into a filled-in *Bgl*II site in pPsA-ΔATG to generate the prespore RLC expression construct pPsA-RLC.

Cell growth and development

All *Dictyostelium* strains were grown in HL-5 medium supplemented with streptomycin at 200 μg/ml. DNA was introduced into *Dictyostelium* cells using electroporation as described in Chen et al. (1995). Strains containing constructs with psA or actin15 promoters were selected with 10 μg/ml G418, while 80 μg/ml G418 was used to select for constructs with ecmA promoters. To initiate development, 4×10^7 cells in 0.25 ml of DB (5 mM Na_2HPO_4, 5 mM KH_2PO_4, 1 mM $CaCl_2$, 2 mM $MgCl_2$) were placed on a pad of filter papers saturated with DB and stored in a moist chamber. For observation with the stereomicroscope, an additional black filter paper was used to facilitate imaging. To observe development of cells containing GFP markers using fluorescence microscopy, cells were developed on a cellophane membrane (BioRad, Hercules CA) saturated with DB and placed on top of a pad of filter papers.

Time-lapse recording of development

Development was monitored with a Zeiss stereomicroscope. Images of developmental structures were collected with a Hamamatsu model 2400 CCD camera at 15 minute intervals using Scion LG-3 frame grabber (Scion Corp., Frederick, MD) and stored as image stacks using the NIH Image program (Wayne Rasband at the US National Institutes of Health and available from the Internet by anonymous ftp from zippy.nimh.nih.gov). GFP-labeled cells in developmental structures were imaged using a Zeiss axioskop through a fluorescein filter set (BP450-490/FT510/LP520). Images were acquired at the desired intervals using a SenSys cooled CCD camera (Photometrics, Tucson AZ) controlled by Zeiss ImagePro software. Images from a time series were converted into an image stack using NIH Image. Image stacks were converted to quick time movies using NIH image program and optimized by Media Cleaner Pro (Terran Interactive, Inc.).

In situ hybridization

In situ hybridizations were performed as described by Escalante and Loomis (1995) with the following modifications: Cells were developed on cellophane membranes (BioRad, Hercules CA) cut to 1 cm discs, saturated with DB on a pad of 4 Whatman #3 filters. Membrane discs containing developmental structures were transferred to a well of a 24-well culture plate filled with methanol. All subsequent steps were also carried out in the same well. Following fixation, the structures were incubated in Proteinase K (GibcoBRL) at 50 μg/ml for 20 minutes. All solutions used in the wash steps were pretreated with diethyl pyrocarbonate (20 μl/500 ml PBS) and autoclaved before use. Digoxigenin-labeled RLC cDNA was prepared using a Boehringer Mannheim digoxigenin DNA Labeling Kit, heat-denatured for 10 minutes prior to hybridization and used at 50 ng/ml. The digoxigenin cDNA was detected with anti-digoxigenin antibody coupled to alkaline phosphatase (Boehringer Mannheim) and visualized with the colorigenic substrates: nitroblue tetrazolium (Sigma) and 5-bromo-4-chloro-3-indolyl phosphate (Sigma). The color reaction was allowed to develop for 1/2 to 1 hour. When satisfactory signal was obtained, the reaction was stopped by washing twice with TE and stored in 80% glycerol. Photomicrography was performed on a Zeiss stereomicroscope.

Western blot analysis and Chemotaxis assays were performed as described previously (Chen et al., 1995).

RESULTS

MlcR$^-$ cells show reduced rates of migration but normal orientation during chemotaxis to cAMP

We have previously shown that, following starvation, cells that

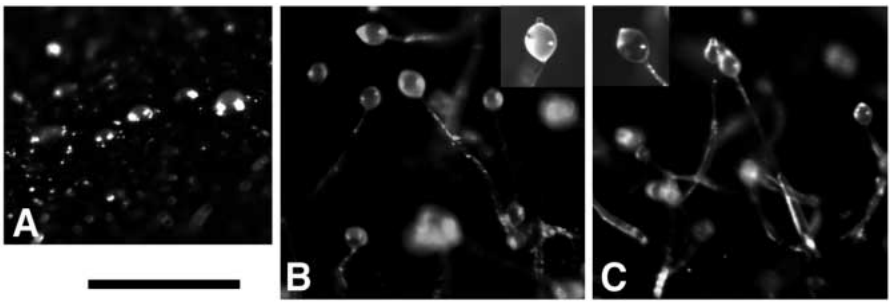

Fig. 1. mlcR⁻/ecmA-RLC cells produce stalks bearing sorocarps carrying reduced numbers of spores. After 26 hours of starvation, mlcR⁻ cells failed to develop beyond mound stage (A), while cells expressing RLC in all cell types throughout development, mlcR⁻/A15-RLC (B) and mlcR⁻/ecmA-RLC (C) formed fruiting bodies. However, the structures formed by mlcR⁻/ecmA-RLC cells contained many additional cells toward the base of the stalk (C), and the sorocarp appears to be largely devoid of spores (compare insets in B and C). Bar, 1 mm.

do not express RLC (mlcR⁻ cells) developed to the mound stage but failed to progress further (Chen et al., 1994, also see Fig. 1A). To analyze their motility, we measured instantaneous velocities and chemotactic orientation in response to a cAMP gradient using a Zigmond chamber assay. Table 1 shows that mlcR⁻ cells exhibited reduced chemotactic motility but were not significantly different from wild type in their ability to orient properly in a cAMP gradient. These results indicate that the primary motility defect in mlcR⁻ cells results from a decreased rate of motility and not a defect in their ability to respond to a cAMP signal.

Expression of RLC exclusively in prestalk cells supports stalk formation but results in mislocalization of spores

The developmental defect of mlcR⁻ cells was fully rescued by constitutive expression of RLC from an actin 15 promoter (mlcR⁻/A15-RLC). Fruiting bodies formed by the mlcR⁻/A15-RLC cell line were indistinguishable from those of wild type (Chen et al., 1994, also see Fig. 1B). Based on these results, we reasoned that expression of RLC in a cell-type-specific manner would allow us to dissect the respective contributions of cell movement in specific cell types during the *Dictyostelium* morphogenetic program. Toward this end, we have engineered *Dictyostelium* RLC null mutants to express RLC under the control of the prestalk promoter, ecmA, or the psA prespore-specific promoter. As can be seen in Fig. 1C, strains expressing RLC exclusively under the control of the ecmA promoter (mlcR⁻/ecmA-RLC) were able to form structures with stalks and apparent sorocarps (Fig. 1C). However, comparison of the mlcR⁻/ecmA-RLC culminants to those formed by mlcR⁻/A15-RLC shows that cells expressing RLC only in prestalk cells generally had thicker stalks and spore cases that were often largely devoid of spores (compare Fig. 1B and C inset). Single sorocarps were assayed for the presence of viable spores by resuspending them in DB containing 0.5% triton and then plated on bacterial lawns. Cells expressing RLC from the ecmA promoter produced only 13% the number of spores as cells expressing the RLC from an actin promoter or wild-type cells. This result suggested that active motility of prestalk cells is not sufficient for culmination and that normal fruiting body formation may require active movement of prespore cells.

To confirm that RLC was expressed in a pattern consistent with that known for the ecmA promoter, we analyzed expression of RLC using western blot analysis and in situ hybridization. In mlcR⁻/ecmA-RLC cells, RLC protein was not detectable prior to 12 hours after starvation using western analysis of whole cell lysates. RLC expression began approximately 12 hours into development and persisted through culmination (Fig. 2A). In situ hybridization was used to determine the spatial pattern of RLC mRNA expression. RLC mRNA was observed at the tip of elongating mounds and fingers (Fig. 2B,C) and retained its anterior localization in migrating slugs and early culminants (Fig. 2D). RLC mRNA can also be found in the posterior prespore zone in lower

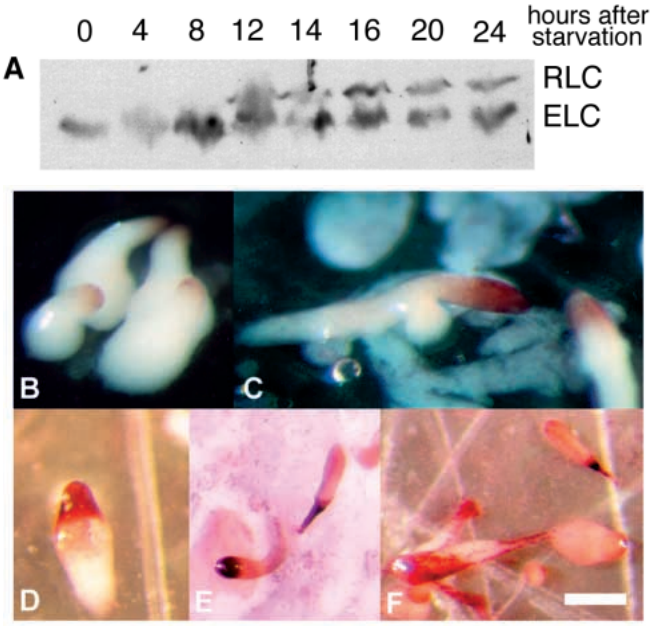

Fig. 2. Expression of RLC in mlcR⁻/ecmA-RLC cells. (A) Western blot of whole cell protein samples taken from different developmental stages of mlcR⁻/ecmA-RLC cells were probed with a polyclonal antibody against myosin. The 16 kDa endogenous myosin essential light chain (ELC) was detected throughout the life cycle, while RLC (expressed from the transgene) was only detectable after 12 hours of starvation. In situ hybridization using RLC cDNA was used to localize RLC mRNA expression throughout development. (B) At 12 hours of development, RLC mRNA appeared at the tip of early fingers. (C) RLC mRNA continued to be expressed primarily in the anterior region of late fingers. (D) RLC mRNA was also localized to anterior of migrating slugs and early culminants. (E) This panel represents an experiment in which color reaction was prolonged to detect expression of RLC in anterior-like cells. RLC mRNA was also found in the prespore zone of early culminants, especially near the areas expected to form lower cup, presumably due to the expression of RLC in ALCs. (F) In fruiting bodies, RLC mRNA appeared at the tip of the sorocarp and along the stalk. Note that at the base of stalk, most of the cells do not express RLC. Bar, 0.25 mm.

Table 1. mlcR⁻ cells exhibit reduced chemotactic motility

	JH10	mlcR⁻ (E12)	mlcR⁻ (E9)
Velocity (μm/min)	12.29±3.62	8.43±2.41	7.26±2.23
Chemotactic Index	0.63±0.29	0.47±0.57	0.58±0.33
n	19	27	21

The chemotactic index was calculated as net displacement in the direction of gradient/total distance traveled. The instantaneous velocity was calculated from the displacement of cells between two video frames captured at 10 second intervals. The value shown is the average of instantaneous velocities over a 10 minute period. n=number of cells analyzed. JH10 is the parental cell line used to create mlcR⁻ cells (Chen et al., 1994). Two mlcR⁻ strains, E9 and E12, were analyzed.

abundance, corresponding to the localization of anterior-like cells (Fig. 2D,E), and at the top of the sorocarp and throughout the stalk of culminants (Fig. 2F). This pattern of RLC expression is consistent with the distribution of ecmA-lacZ, the marker used to define prestalk A and prestalk O cell types (Jermyn and Williams, 1991; Early et al., 1993; Chen et al., 1995).

To determine how expression of RLC in pstA/pstO cells affected the ability of prestalk cells to localize, ecmA-GFP-expressing cells were mixed with wild-type cells in a 1:50 to 1:10 ratio and developed to the slug stage. Fig. 3 shows that the tagged RLC null mutants localized well behind the normal prestalk zone of the slug (Fig. 3B), while cells expressing RLC under the control of either the actin promoter or ecmA promoter localized normally to the anterior end of the slug. Note that, although the ecmA GFP signal was clearly seen in the prestalk region in ecmA-RLC cells, the cells did not extend completely to the tip as they did in actin-RLC cells. This suggests that, although ecmA-driven expression of RLC restored ecmA-GFP localization to the prestalk region of the slug, the rescue may not be complete. Nonetheless, reasonable stalk formation was observed. In contrast, ecmA-GFP localization of cells expressing RLC from the prespore promoter, psA, was similar to the RLC null mutant (compare Fig. 3B and D).

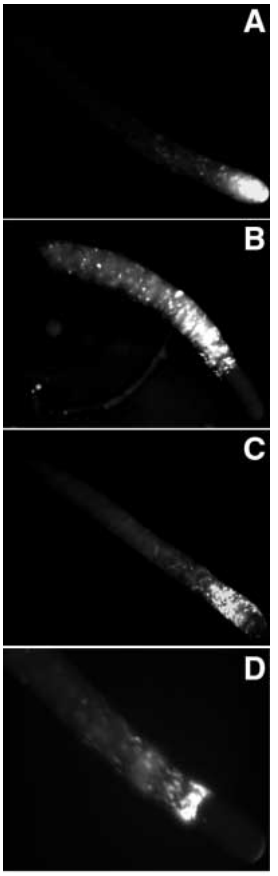

Fig. 3. Prestalk cell localization is restored by expression of RLC from the ecmA promoter, but not the psA promoter. Cells expressing GFP from the ecmA promoter were mixed 1:50 with wild-type cells and developed to the slug stage. (A) ecmA-GFP-labeled cells expressing RLC from the actin promoter; (B) ecmA-GFP-labeled cells in mlcR- cells; (C) ecmA-GFP labelled cells expressing RLC from the ecmA promoter; (D) ecmA-GFP-labeled cells expressing RLC from the psA promoter.

Prespore cells in mlcR⁻/ecmA-RLC early culminants fail to move to the top of extending stalks

To monitor the cell movements that occur during culmination, we collected time-lapse video images of culminating cell aggregates. Fig. 4 shows the early stages of culmination for mlcR⁻/A15-RLC taken from a typical time-lapse video. (The time-lapse video sequences are available over the internet at http://dicty.cmb.nwu.edu/movies/chen.html.) At the onset of culmination, wild-type preculminants (Fig. 4A) extended no more than two fold in length before the posterior prespore mass began to round up near the base of the culminant (Fig. 4B,C). As culmination progressed, the distance between the substrate and the base of the rounded prespore mass increased and the most posterior region of the prespore zone contracted toward the more anterior regions. This posterior domain of the prespore zone appeared to move as a coordinated unit that maintained its position at the tip of the elongating culminant (Fig. 4D-H). To follow movement of prespore cells in living culminants, we marked the prespore cells by expressing GFP using the psA promoter (Early and Williams, 1989). Wild-type cells containing the psA-gfp marker were mixed with unlabeled wild-type cells at a 1:10 ratio to facilitate visualizing individual labeled cells. Time-lapse movies of the fluorescence images revealed that prespore cells in the control culminants exhibit rotational movement while ascending the stalk (http://dicty.cmb.nwu.edu/movies/chen.html). The rotational motion can be observed most often in the posterior prespore zone but sometimes occurred throughout the prespore zone. In Fig. 4I, the frames of this sequence have been superimposed to show the tracks of cell movement. The tracks followed by most cells in this culminant exhibited an approximate 45° angle to the long axis of the culminant.

Fig. 5 shows frames from a time-lapse movie of a typical mlcR⁻/ecmA-RLC early culminant. The posterior prespore zone never showed the rounding of the base and a majority of the prespore mass was never observed to move up the extending stalk (Fig. 5A-C). The mlcR⁻/ecmA-RLC culminants continued elongating as the stalk extended and became a finger-like structure (Fig. 5B-E). Eventually, the prespore zone broke apart in the middle as elongation of the stalk extended beyond the limit of the prespore zone extension (Fig. 5F). The most anterior portion of the prespore zone was

carried by the stalk and formed a sorus that contained significantly fewer spores than wild type, while the lower portion of the prespore zone remained at the base of stalk (Fig. 5G,H). The prespore cells in mlcR⁻/ecmA-RLC culminants marked by psA-gfp, did not exhibit the rotational motion typical of wild-type prespore cells. Instead, the prespore cells exhibited movements parallel to the long axis of the culminant with no obvious rotation and greatly reduced overall movement at the posterior prespore zone (http://dicty.cmb.nwu.edu/movies/chen.html). The paths of cell movement are shown in the overlay in Fig. 5I. The culminant in this figure corresponds to the stage shown in Fig. 5D. The posterior prespore zone failed to catch up with the forward movement of the more anterior portion of prespore zone perhaps due to the absence of rotational movement and the reduced velocity of cells lacking RLC expression. This forward movement, most likely generated by the force of the extending stalk, eventually led to the splitting of the prespore zone.

MlcR⁻ cells expressing RLC exclusively in prespore cells fail to form stalks

Since it appeared that normal morphogenesis required a component of active prespore cell motility, we next characterized morphogenesis of mlcR⁻ cells expressing RLC from a prespore-specific promoter, psA (Early and Williams, 1989). Following starvation, the prespore RLC expression strain, mlcR⁻/psA-RLC, formed balloon-shaped structures (Fig. 6A,B). Occasionally these balloon structures elongated into very short but thick migrating slugs (Fig. 6A,B). Time-lapse observation showed that the mlcR⁻/psA-RLC mounds often first extended into short and thick fingers (Fig. 6C-E). As development progressed, the tip of the fingers waved around suggesting significant motion was occurring within the structure. The rounded balloon-like end of the finger eventually collapsed back toward the substratum (Fig. 6F-H). These movements were similar to the rounding up and contraction of the prespore zone observed in wild-type cells but which were absent in the developing mlcR⁻/ecmA-RLC cells. The balloon structure appears similar to a sorus. However, in the absence of myosin function in the prestalk cells, stalk formation did not occur, effectively stranding the sorus on the surface.

Examination of the temporal and spatial pattern of RLC expression in mlcR⁻/psA-RLC cells using both western immunoblot analysis and in situ hybridization confirmed that the RLC was expressed in a pattern similar to that observed for prespore cell localization. The mlcR⁻/psA-RLC cells did not express detectable levels of RLC protein until 12 hours after starvation (Fig. 7A). At this developmental stage, in situ hybridization localized RLC mRNAs to the lower regions of mound (Fig. 7B) – a pattern typical of prespore-specific expression. Similarly, RLC mRNA was localized to the posterior region in early fingers (Fig. 7C) and many 'balloon' structures (Fig. 7D). However, in some 'balloon' structures, RLC mRNA was found to exhibit a more anterior localization (Fig. 7E).

To determine how expression of RLC from the psA promoter affected prespore cell localization in slugs, psA-GFP-expressing cells were mixed with wild-type cells in a 1:50 to 1:10 ratio and allowed to develop to the slug stage. Fig. 8 shows that, while the tagged RLC null mutants localized to the posterior end of the prespore zone, cells expressing RLC under the control of either the actin promoter or psA promoter localized normally throughout the prespore zone of the slug (Fig. 8A,C). In contrast, psA-GFP localization of cells expressing RLC from the prestalk promoter, ecmA, was similar to the RLC null mutant (compare Fig. 8B and D). This result suggests that psA-driven expression of RLC restores the normal localization of prespore cells, while ecmA expression does not.

Prespore cells move upwards in mlcR⁻/psA-RLC cells in the absence of stalk extension

The observed patterns of RLC localization in the developing mlcR⁻/psA-RLC cells suggested the possibility that prespore cells in these balloon structures might move from their initial position near the base of the aggregate toward the tops of the balloon structures much as they might move up a stalk. We have again followed prespore movement using the psA-gfp prespore marker. Time-lapse video images of mlcR⁻/psA-RLC cells that also expressed GFP driven by the psA promoter were recorded. Fig. 9 shows frames from a typical

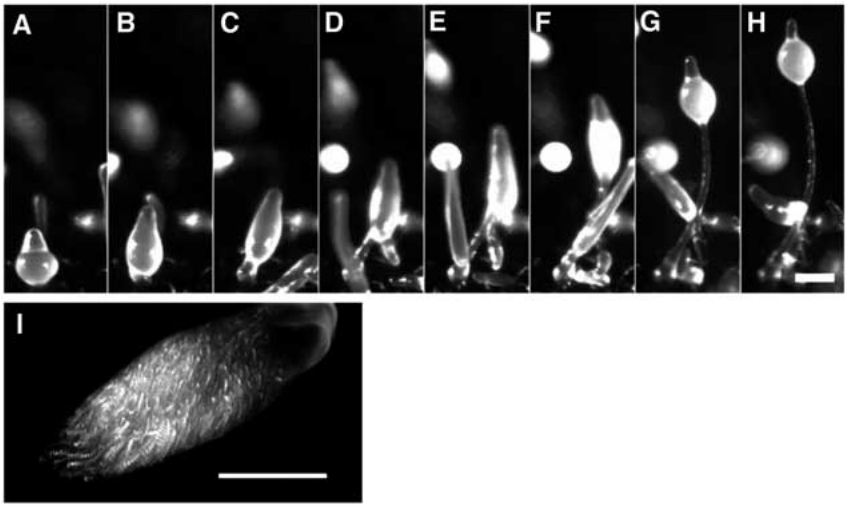

Fig. 4. Early culminants of cells expressing RLC in all cell types (mlcR⁻/A15RLC) showed normal movement of the prespore zone up the extending stalk in a well coordinated, spiraling motion. (A-H) Each panel in this series of stereoscopic images was captured at 40-minute intervals from a typical control culminant (except the interval between E and F, which is 30 minutes). (A) At 21 hours after starvation, a preculminant is at the onset of culmination. (B) Before the stalk emerged from the bottom, the early culminant elongated. (C) The prespore zone can be seen rising from the surface exposing stalk below the prespore mass. (D-H) The prespore mass went through slight shape change but always moved as a coordinated unit on top of the extending stalk. (I) Overlay of a fluorescence image series of GFP-labeled prespore cells in a control culminant at a developmental stage similar to the culminant in C. 20 frames were captured at 1 minute intervals, and cells in this culminant can be seen to follow a path at a 45° angle to the long axis of the culminant indicative of the spiral motion that can be clearly observed in animation of these frames. Bar, 0.25 mm.

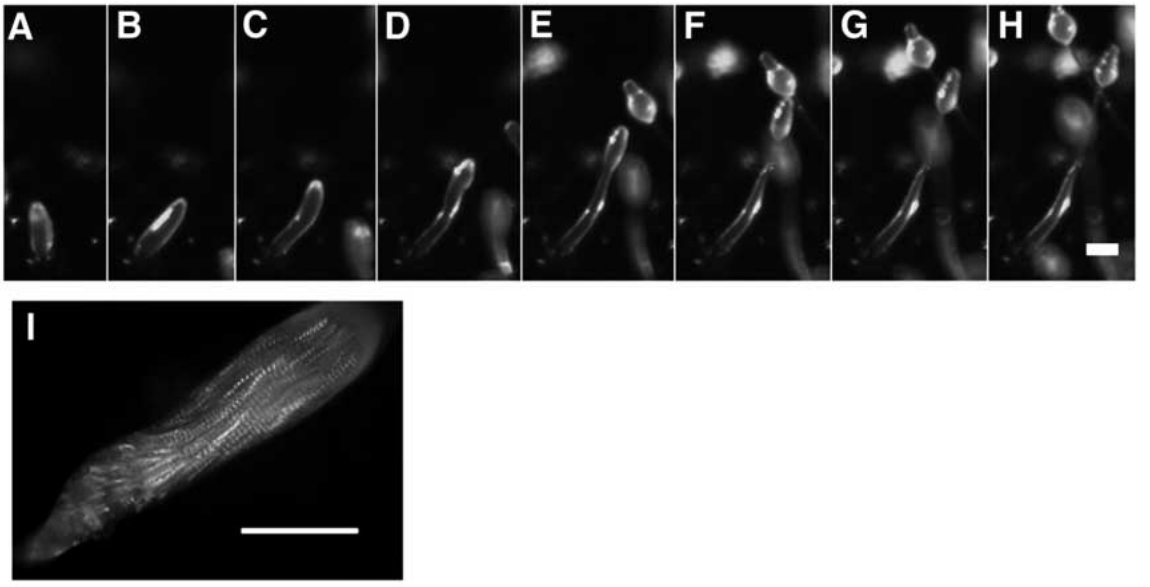

Fig. 5. Prespore zone of mlcR^{-}/ecmA-RLC early culminants failed to move up the extending stalk. (A-H) This time series of a typical mlcR^{-}/ecmA-RLC culminant is composed of images captured 45 minutes apart starting at 20 hours after starvation. (A) A preculminant that just began culmination appeared similar to a control preculminant (compare with Fig. 4B for example). (B-E) The prespore zone did not ascend the extending stalk as an oblong shaped mass seen in control culminant. Instead, the whole culminant stretched along with the extending stalk tube into a finger-like appearance. (F-H) The stalk tube eventually extended to break the prespore zone and carried the top portion of the prespore mass along while leaving the remainder of the prespore zone at the base of the stalk. (I) Overlay of a fluorescence image series of GFP-labeled prespore cells in a mlcR^{-}/psA-RLC culminant equivalent to the stage as the culminant in D. When 25 consecutive frames captured at 2 minute intervals are overlaid, cells in this culminant can be seen to follow a path parallel to the long axis of the culminant. Note the relatively poor motility of the prespore cells at the base of the culminant (compare with Fig. 4I). Bar, 0.25 mm.

'balloon' structure as development progresses. As can be seen from this series, with time the GFP signal moved from the base toward the top of the structure. The GFP cells appeared to move toward the top in a spiral motion which can be most easily seen in the video sequence (http://dicty.cmb.nwu.edu/movies/chen.html). These results indicate that, even in the absence of normal stalk formation, prespore cells exhibit a strong movement toward the tip. In addition, the contraction that produced the rounding of the base can be clearly seen.

DISCUSSION

Dictyostelium development provides a particularly good experimental system to study the role of cell movements during morphogenesis. Mutants defective in both cell-cell signaling (Dharmawardhane et al., 1994; Firtel, 1996; Mann et al., 1997; Okaichi et al., 1992; Pitt et al., 1992; Segall et al., 1995) and cytoskeletal elements (Haugwitz et al., 1994; Rivero et al., 1996; Witke et al., 1992) have been shown to display abnormal morphogenesis. Several studies have shown the importance of myosin for normal morphogenesis (DeLozanne and Spudich, 1987; Knecht and Loomis, 1987; Wessels et al., 1988; Elliot et al., 1993, Traynor et al., 1994; Springer et al., 1994; Chen et al., 1994, 1995). In this report, we have used cell-type-specific expression of RLC in RLC knockouts to produce strains in which the functional defects in myosin, caused by a lack of RLC, have been rescued selectively in specific cell types during development. These strains have enabled us to define the role

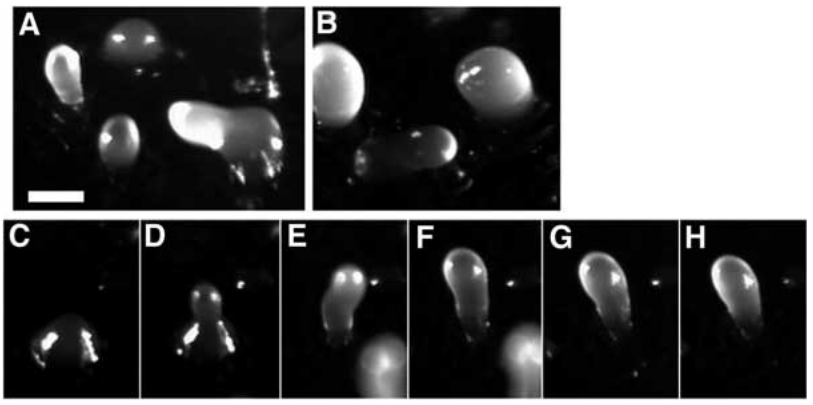

Fig. 6. MlcR^{-}/psA-RLC cells do not form stalks, but form sorocarp-like structures. (A,B) After 16 hours of starvation, the most common structures formed by mlcR^{-}/psA-RLC cells looked like balloons. A migrating slug can occasionally be seen to emerge from a balloon-like structure (A). (C-H) Formation of a 'balloon' from mound. (The interval between C,D; E,F; G,H is 60 minutes; D and E are 90 minutes apart and F and G are 120 minutes apart.) (C) mlcR^{-}/psA-RLC mounds at 14 hours of development. (D) The mound elongates into a short, stubby finger. (E) During development, the tip kept changing direction producing the crooked appearance of the finger. (F) The tip of the finger enlarged as elongation ceased. (G,H) The terminal phenotype typically shows a balloon-like structure. Bar, 0.25 mm.

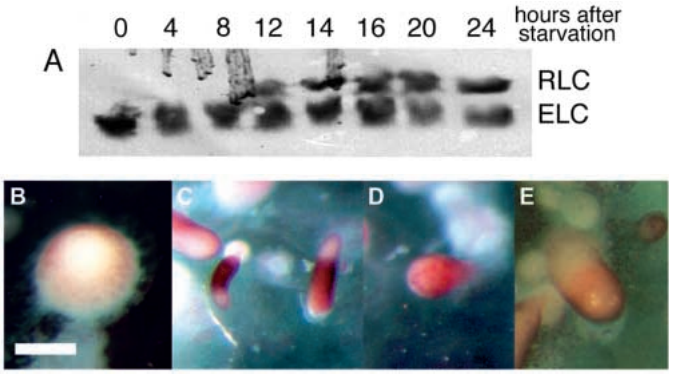

Fig. 7. Expression of RLC in mlcR$^-$/psA-RLC cells. (A) Western blot of whole cell protein samples from different developmental stages of mlcR$^-$/psA-RLC cells were probed with a polyclonal antibody against myosin. The endogenous 16 kDa myosin essential light chain (ELC) was detected throughout the life cycle, while RLC expressed from the transgene was only detectable after 12 hours of starvation. In situ hybridization using RLC cDNA was used to detect RLC mRNA expression. At 12 hours of development, RLC mRNA appeared at the lower portion of the mound (B). RLC mRNA also appeared at the posterior portion of early fingers (C) and some of the round ball structures (D). RLC mRNA was also found on the anterior portion of some balloon-like structures (E). Bar, 0.25 mm.

of myosin-dependent cell motility in the major cell types established during *Dictyostelium* development. Restoring myosin function in prestalk cells was sufficient to produce stalks with sorocarps atop them. However, the sorocarps contained greatly reduced numbers of spores, and the stalks had an abnormal accumulation of prespore cells and spores surrounding their base. In contrast, prespore-specific expression of RLC was unable to support production of stalks. In the absence of functional myosin in prestalk cells, mlcR$^-$/psA-RLC mounds elongated inefficiently to form aberrant fingers, which then collapsed into balloon-like structures that resembled sorocarps which had been stranded on the substrate. These observations provide evidence for a critical role of myosin function in both prespore and prestalk cells in mediating morphogenetic events from mound to culmination.

It has been shown by several investigators that cells in a mound exhibit rotational movement (Clark and Steck, 1979; Elliot et al., 1993; Siegert et al., 1994). It has been proposed that this rotational movement, thought to be organized by a cAMP chemotactic response, persists into the emerging tip. This movement has been suggested to drive the extension of the tip to form fingers (Clark and Steck, 1979). In mlcR$^-$/ecmA-RLC mounds, restoring myosin function in prestalk cells was sufficient to allow efficient finger formation. In contrast, when RLC was expressed in prespore cells, only short and often crooked fingers were observed, suggesting that prestalk cell movement may drive tip and finger formation. Although we have not yet characterized cell movement in detail at this stage, it is tempting to speculate that prestalk-specific expression of RLC restores the nearly normal rotational movement in the mounds.

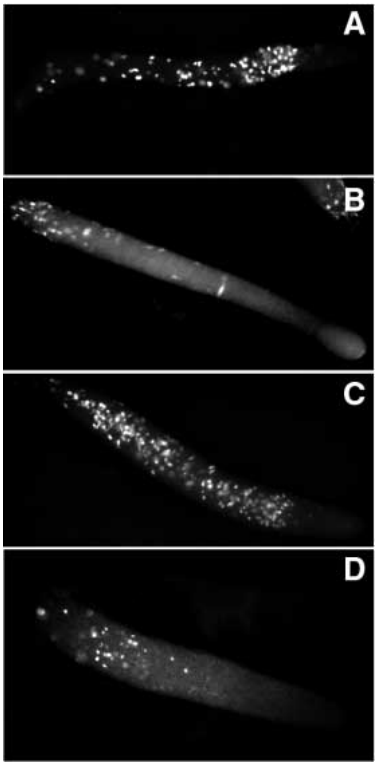

Fig. 8. Prespore cell localization is restored by expression of RLC from the psA promoter, but not the ecmA promoter. Cells expressing GFP from the psA promoter were mixed 1:50 with wild-type cells and developed to the slug stage. (A) psA-GFP-labeled cells expressing RLC from the actin promoter; (B) psA-GFP-labeled cells in mlcR$^-$ cells; (C) psA-GFP labelled cells expressing RLC from the psA promoter; (D) psA-GFP-labeled cells expressing RLC from the ecmA promoter.

Prestalk cells have been proposed to provide the major motive force for slug movement (Inouye and Takeuchi, 1980; Williams et al., 1986). Myosin localization to the cortex of anterior cells and posterior peripheral cells in migrating slugs has been interpreted to suggest that myosin plays an important role in this slug migration (Elliot et al., 1991). An alternative model has proposed that prespore cells are responsible for active slug movement. This suggestion was based on the observation that prestalk cells exhibited a rotational movement

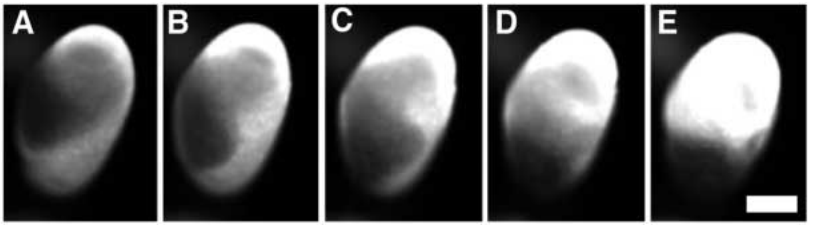

Fig. 9. Prespore cells undergo rotational ascending motion in mlcR$^-$/psA-RLC 'balloon' structure. Marked by psA-gfp, the prespore zone in a mlcR$^-$/psA-RLC 'balloon' was originally localized primarily to the lower portion of the structure. At start of recording, a portion of the prespore zone in this 'balloon' had reached the top of the structure (A). Each panel is 20 minutes apart. (B-D) The prespore zone can be seen to move upward in a spiral motion from left toward the right. (E) After 100 minutes, most of the prespore cells were at the top. Bar, 0.1 mm.

perpendicular to the direction of slug migration while prespore cells moved in the direction of slug migration in a coherent periodic fashion (Siegert and Weijer, 1992; Dormann et al., 1996). We have observed that mlcR$^-$/ecmA-RLC strains were able to form migrating slugs (data not shown), supporting the role of prestalk cell motility in slug migration. On the contrary, cells expressing RLC exclusively in prespore cells were also observed to form migrating slugs with lower frequency, suggesting a minor role for prespore motility in slug migration.

It has been widely accepted that the driving force behind *Dictyostelium* culmination is the downward movement of prestalk cells as they mature into stalk cells and form a cellulose encased stalk tube. In this scheme, the prespore/spore mass is passively lifted from the substrate by extension of the stalk tube (see Durston et al., 1976; Jermyn and Williams, 1991). Our observations during culmination of mlcR$^-$/ecmA-RLC cells lines suggest that two independent processes requiring active movement of both prestalk and prespore cells contribute to the formation of normal fruiting bodies. The ability of cells expressing myosin only in prestalk cells to form a stalk with a sorocarp at the top supports the importance of stalk formation in the process. However, the greatly reduced numbers of spores in the sorocarp, along with the large number of prespore/spore cells found near the base of the stalk in these culminants also points to an important role for movement of prespore cells during culmination. In order to form a complete fruiting body, a culminant not only needs to construct a stalk that lifts the sorocarp above the substratum, it also requires myosin-dependent contractility and/or motility for prespore cells to move to the top of the stalk during early phase of culmination.

An important clue regarding the nature of the myosin dependent process required for normal placement of spores comes from the observation of mounds expressing RLC in prespore cells. These structures display a constriction of their base allowing it to assume the oblong shape seen as the prespore mass begins to move upwards. A similar constriction is seen in wild-type culminants. In contrast, mounds expressing RLC in prestalk (pstA and pstO) cells do not produce this constriction. This constriction at the base of prespore zone may result from the spiraling motion of the posterior prespore cells, which act to compress the prespore zone. The slime sheath surrounding the prespore mass may then reorganize to reinforce the constriction. Alternatively, the constriction may represent a specialized contractile event produced by myosin bearing cells at the surface of the cell mass (Elliot et al., 1991). A population of prestalk-like cells known as anterior-like cells (ALCs) has been postulated to participate in moving the spore/prespore cells atop the stalk (Sternfeld and David, 1982). Prior to culmination, a population of the ALCs moves to the base of culminants to form a supporting structure for the sorocarp known as the ‘lower cup’ (Dormann et al., 1996; Jermyn and Williams, 1992; Sternfeld and David, 1982). It seems unlikely that the lower cup is responsible for the upward movement of the spore/prespore cells, since we have observed expression of RLC in anterior-like cells in mlcR$^-$/ecmA-RLC culminants, yet many spore/prespore cells failed to reach the top of the stalk. The rotational movement of prespore cells that we have observed in mlcR$^-$/psA-RLC balloon-like structures shows that the prespore cell motility can occur in the absence of stalk extension. These results suggest that movement of prespore cells during the early stages of culmination is an independent event from stalk extension. Based on these observations, we propose that the prespore cells participate in two types of motility during culmination: constriction of the base and upward rotational movement along the extending stalk.

We have previously described ELC knockout lines in which mounds appear to have two different developmental phenotypes (Chen et al., 1995). Approximately half of the mounds failed to progress beyond the mound stage in a fashion similar to mlcR$^-$ and mhcA$^-$ mutants. The other half of the mounds formed fruiting bodies that retained a significant proportion of their prespore cells in a cone around the base – a morphology identical to that observed in these studies for cells expressing RLC only in prestalk cells. We have interpreted the variability of mlcE$^-$ morphology as a threshold effect, in which some mlcE$^-$ mounds have sufficient motility or contractile function to progress past the mound stage. The observation that mlcR$^-$/ecmA-RLC cells produce similar structures to mlcE$^-$ mounds that exceed this threshold suggests that the prespore motility required for normal culmination is more sensitive to reduced myosin function than is prestalk motility.

The single-cell chemotactic response of mlcR$^-$ cells resembles that of mlcE$^-$ cells. Both strains were able to orient in a cAMP gradient, showing good chemotactic indices, but they both exhibited reduced rates of cell movement. However, during multicellular development, mlcR$^-$ cells became arrested at the same stage as mhcA$^-$ cells while a subset of mlcE$^-$ mounds progressed further in the developmental program. A clue to understanding the different developmental phenotypes may come from the different degrees of myosin localization defects observed for these three strains. The mhcA$^-$ cells completely lacked myosin thick filaments while a significant portion of the myosin in mlcR$^-$ cells appeared abnormally localized and lacked enzymatic activity (Chen et al., 1994). In contrast, mlcE$^-$ cells contained normally localized but enzymatically inactive myosin (Chen et al., 1995). This suggests that the normally localized myosin thick filaments may contribute to the increased developmental potential of the mlcE$^-$ cells compared to mlcR$^-$ and mhcA$^-$ cells. The ability to polarize normally suggests that the cell shape changes necessary for normal chemotaxis of single cells occurs normally in both mlcE$^-$ and mlcR$^-$ cells. Optimal movement rates, however, depend on motor function of myosin, and therefore, the light chain mutants were less efficient in chemotaxis. During multicellular development, similar chemotactic responses toward cAMP waves have been proposed to govern cell movement and differentiation (Clark and Steck, 1979; Siegert and Weijer, 1992). Movement in the context of development adds the additional influences resulting from interactions with neighboring cells such as cell-cell adhesion and the necessity to overcome traction forces between cells. Although mlcR$^-$ single cells exhibited chemotactic response similar to mlcE$^-$ cells, they fail to penetrate into the aggregation stream of wild-type or mlcE$^-$ cells (Xu et al., unpublished data). In addition, mlcR$^-$ cells also exhibit aberrant patterns of movement in mounds (Gollin and McNally, Washington University, personal communication). Taken together, these results suggest that the abnormal myosin localization of mlcR$^-$ cells is unable to support efficient

movement of mlcR$^-$ cells in the context of multicellular structures.

In conclusion, this study has used cell-type-specific expression of RLC in a RLC knockout to manipulate motile functions of specific cell types during *Dictyostelium* development. This approach has identified two distinct myosin-dependent motile functions that are required for normal culmination. The approach used in these studies provides a direct means of assessing the role of cell motility in distinct cell types during a morphogenetic program and may be useful in developmental studies of other organisms.

This work was supported by NIH Grant ROI GM39214.

REFERENCES

Chen, P., Ostrow, B. D., Tafuri, S. R. and Chisholm, R. L. (1994). Targeted disruption of the Dictyostelium RMLC gene produces cells defective in cytokinesis and development. *J. Cell Biol.* **127,** 1933-1944.

Chen, T.-L. L., Kowalczyk, P. A., Ho, G. and Chisholm, R. L. (1995). Targeted disruption of the Dictyostelium myosin essential light chain gene produces cells defective in cytokinesis and morphogenesis. *J. Cell Sci.* **108,** 3207-3218.

Clark, R. L. and Steck, T. L. (1979). Morphogenesis in Dictyostelium: An orbital hypothesis. *Science* **204,** 1163-1168.

Dharmawardhane, S., Cubitt, A. B., Clark, A. M., and Firtel, R. A. (1994). Regulatory role of the G alpha 1 subunit in controlling cellular morphogenesis in Dictyostelium. *Development* **120,** 3549-3561**.**

DeLozanne, A. and Spudich J. A. (1987). Disruption of the *Dictyostelium* myosin heavy chain gene by homologous recombination. *Science* **236**, 1086-1091.

Devreotes, P. (1989). Dictyostelium discoideum: a model system for cell-cell interactions in development. *Science* **245**, 1054-1058.

Dormann, D., Siegert, F. and Weijer, C. J. (1996). Analysis of cell movement during the culmination phase of Dictyostelium development. *Development* **122**, 761-769.

Durston, A. J., Cohen, M. H., Drage, D. J., Potel, M. J., Robertson, A. and Wonio, D (1976). Periodic movements of Dictyostelium discoideum sorocarps. *Dev. Biol.* **52**, 173-180.

Early, A. E., Gaskell, M. J., Traynor, D. and Williams, J. G. (1993). Two distinct populations of prestalk cells within the tip of the migratory Dictyostelium slug with differing fates at culmination. *Development* **118**, 353-362.

Early, A. E. and Williams, J. G. (1989). Identification of DNA sequences regulating the transcription of a Dictyostelium gene selectively expressed in prespore cells. *Nucleic Acids Res.* **17,** 6473-6484.

Elliot, S., Vardy, P. H. and Williams, K. L. (1991). The distribution of Myosin II in Dictyostelium discoideum slug cells. *J. Cell Biol.* **115**, 1267-1274.

Elliot, S., Joss, G. H., Spudich, A. and Williams, K. L. (1993). Patterns in Dictyostelium discoideum: the role of myosin II in the transition from the unicellular to the multicellular phase. *J. Cell Sci.* **104**, 457-466.

Escalante, R. and Loomis, W. F. (1995). Whole-mount in situ hybridization of cell-type-specific mRNAs in Dictyostelium. *Dev. Biol.* **171,** 262-266.

Firtel, R. A. (1996). Interacting signaling pathways controlling multicellular development in Dictyostelium. *Curr. Opin. Genet. Dev.* **6**, 545-554.

Haugwitz, M., Noegel, A. A., Karakesisoglou, J. and Schleicher, M. (1994). Dictyostelium amoebae that lack G-actin-sequestering profilins show defects in F-actin content, cytokinesis, and development. *Cell* **79**, 303-314.

Harwood, A. J. and Drury, L. (1990). New vectors for expression of the E. coli lacZ gene in Dictyostelium. *Nucleic Acids Res*. **18**, 4292.

Inouye, K. and Takeuchi, I. (1980). Motive force of the migrating pseudoplasmodium of the cellular slime mould Dictyostelium discoideum. *J. Cell Sci.* **41,** 53-64.

Jermyn, K. A. and Williams, J. G. (1991). An analysis of culmination in Dictyostelium using prestalk and stalk-specific cell autonomous markers. *Development* **111**, 779-787.

Knecht, D. A. and Loomis, W. F. (1987). Antisense RNA inactivation of myosin heavy chain gene expression in *Dictyostelium discoideum*. *Science* **236**,1081-1085.

Mann, S. K., Brown, J. M., Briscoe, C., Parent, C., Pitt, G., Devreotes, P. N. and Firtel, R. A. (1997). Role of cAMP-dependent protein kinase in controlling aggregation and postaggregative development in Dictyostelium. *Dev. Biol.* **183,** 208-221**.**

Okaichi, K., Cubitt, A. B., Pitt, G. S. and Firtel, R. A. (1992). Amino acid substitutions in the Dictyostelium G alpha subunit G alpha 2 produce dominant negative phenotypes and inhibit the activation of adenylyl cyclase, guanylyl cyclase, and phospholipase C. *Mol. Biol. Cell* **3**, 735-747**.**

Pitt, G. S., Milona, N., Borleis, J., Lin, K. C., Reed, R. R. and Devreotes, P. N. (1992). Structurally distinct and stage-specific adenylyl cyclase genes play different roles in Dictyostelium development. *Cell* **69,** 305-315**.**

Rivero, F., Koppel, B., Peracino, B., Bozzaro, S., Siegert, F., Weijer, C. J., Schleicher, M., Albrecht, R. and Noegel, A. A., (1996). The role of the cortical cytoskeleton: F-actin crosslinking proteins protect against osmotic stress, ensure cell size, cell shape and motility, and contribute to phagocytosis and development. *J. Cell Sci.* **109,** 2679-2691**.**

Segall, J. E., Kuspa, A., Shaulsky, G., Ecke, M., Maeda, M., Gaskins, C., Firtel, R. A. and Loomis, W. F. (1995). A MAP kinase necessary for receptor-mediated activation of adenylyl cyclase in Dictyostelium. *J. Cell Biol.* **128,** 405-413**.**

Siegert, F. and Weijer, C. J. (1992). Three-dimensional scroll waves organize Dictyostelium slugs. *Proc. Natl. Acad. Sci. USA* **89,** 6433-6437.

Siegert, F., Weijer, C. J., Nomura, A. and Miike, H. (1994). A gradient method for the quantitative analysis of cell movement and tissue flow and its application to the analysis of multicellular Dictyostelium development. *J. Cell Sci.* **107,** 97-104.

Springer, M. L., Patterson, B. and Spudich, J. A. (1994). Stage-specific requirement for myosin II during Dictyostelium development. *Development* **120**, 2651-2660.

Sternfeld, J. and David, C. N. (1982). Fate and regulation of anterior-like cells in Dictyostelium slugs. *Dev. Biol*. **93,** 111-118.

Traynor, D., Tasaka, M., Takeuchi, I. and Williams, J. (1994). Aberrant pattern formation in myosin heavy chain mutants of Dictyostelium. *Development* **120**, 591-601.

Wessels, D., Soll, D. R., Knecht, D., Loomis, W. F., DeLozanne, A. and Spudich, J. A. (1988). Cell motility and chemotaxis in Dictyostelium amoebae lacking myosin heavy chain. *Dev. Biol*. **128**, 164-177.

Wessels, D., Murray, J. and Soll, D. R. (1992). Behavior of Dictyostelium amoebae is regulated primarily be the temporal dynamic of the natural cAMP wave. *Cell Motil. Cytoskel*. **23,** 145-156.

Williams, K. L., Vardy, P. H. and Segel, L. A. (1986). Cell migrations during morphogenesis: some clues from the slug of Dictyostelium discoideum. *BioEssays* **5,** 148-152.

Witke, W., Schleicher, M. and Noegel, A. A. (1992). Redundancy in the microfilament system: abnormal development of Dictyostelium cells lacking two F-actin cross-linking proteins. *Cell* **68,** 53-62.